

Supporting information

Insight into swift heavy ion radiation response of $\text{Y}_3\text{Al}_5\text{O}_{12}$ and Nd^{3+} - $\text{Y}_3\text{Al}_5\text{O}_{12}$: Structural damage and defect dynamics

Koushik Bhandari,^{a,f} V. Grover,^{*b,f} P. Kalita,^c K. Sudarshan,^{d,f} B. Modak,^{b,f} Saurabh K Sharma,^e P. K. Kulriya^e

^aRadiometallurgy Division, Bhabha Atomic Research Centre, Mumbai- 400085, India

^bChemistry Division, Bhabha Atomic Research Centre, Mumbai- 400085, India

^cSchool of Engineering, University of Petroleum & Energy Studies, Dehradun- 248007, India

^dRadiochemistry Division, Bhabha Atomic Research Centre, Mumbai- 400085, India

^e School of Physical Sciences, Jawahar Lal Nehru University, New Delhi- 110067, India

^fHomi Bhabha National Institute, Mumbai- 400094, India

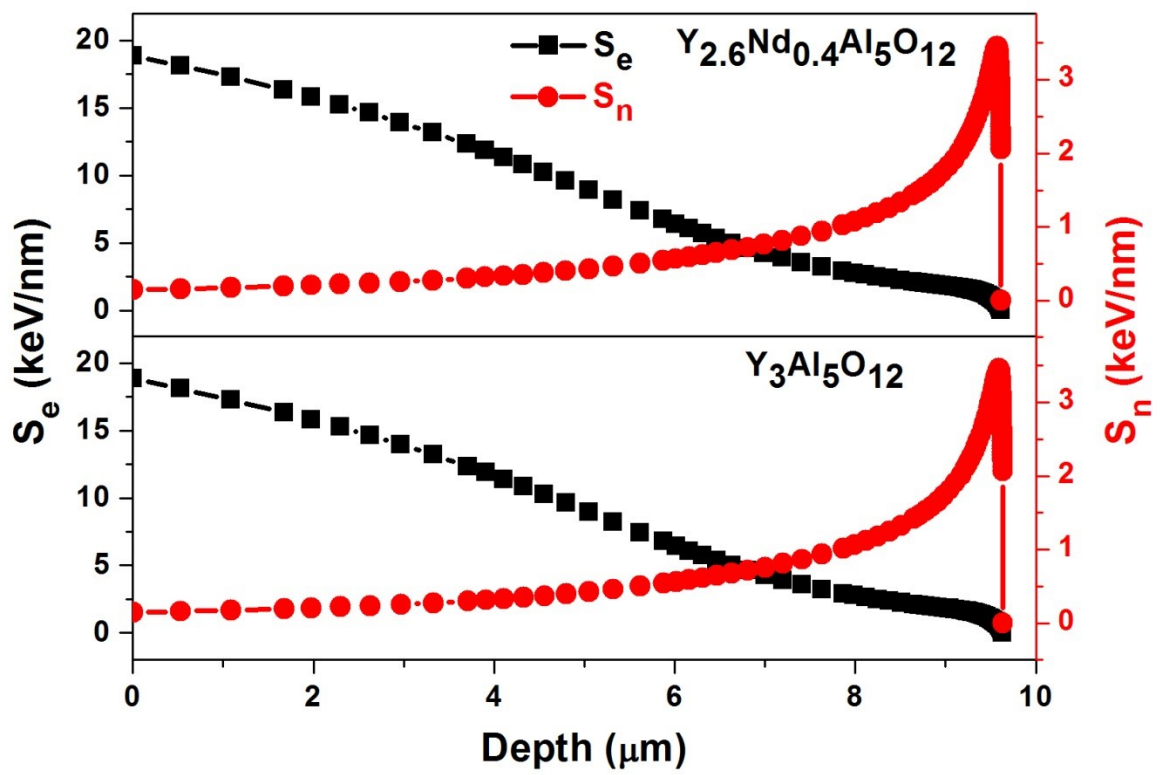


Fig. S1: Depth profile of electronic stopping power (S_e), nuclear stopping powers (S_n) of 100 MeV I ions in $\text{Y}_3\text{Al}_5\text{O}_{12}$ and $\text{Y}_{2.6}\text{Nd}_{0.4}\text{Al}_5\text{O}_{12}$.

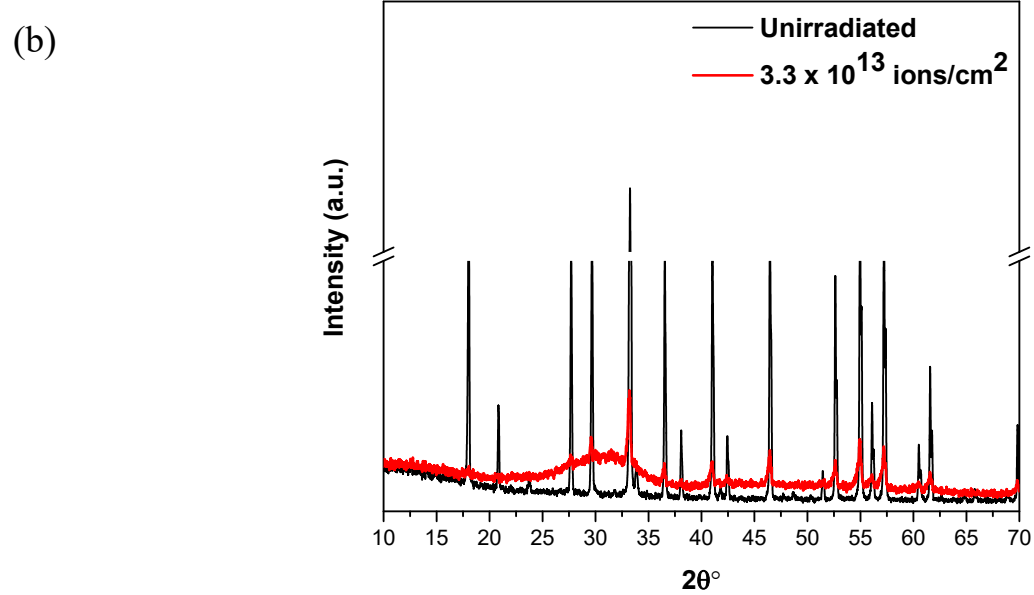
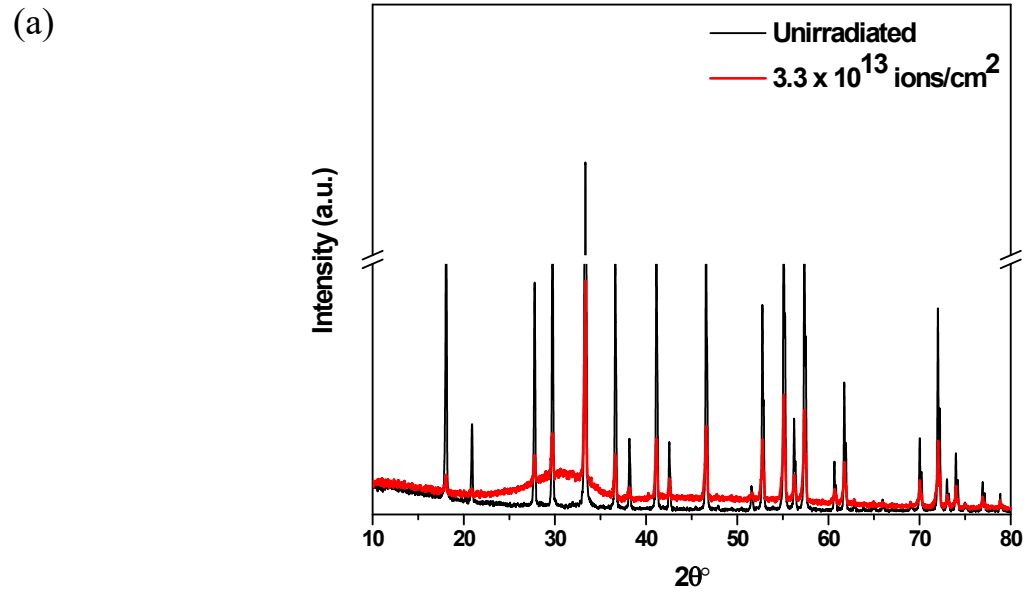
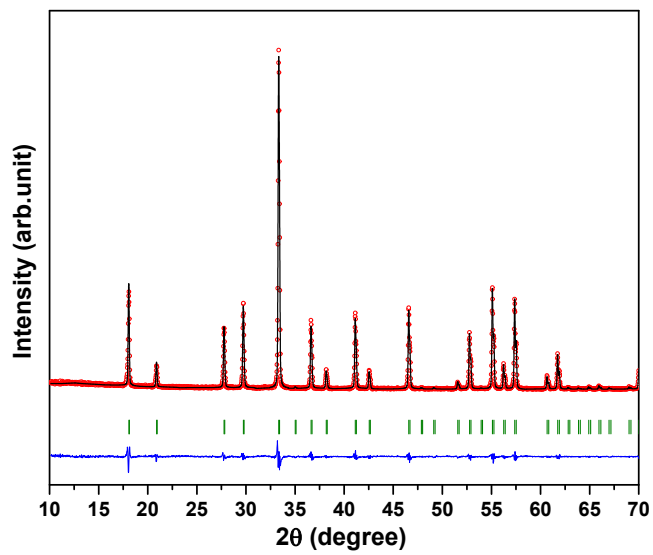


Fig. S2: Broad hump at $\sim 2\theta = 20^\circ$ - 40° for (a) $\text{Y}_3\text{Al}_5\text{O}_{12}$ and (b) $\text{Y}_{2.6}\text{Nd}_{0.4}\text{Al}_5\text{O}_{12}$ indicates coexistence amorphous phase with crystalline phase after irradiation.

(a)



(b)

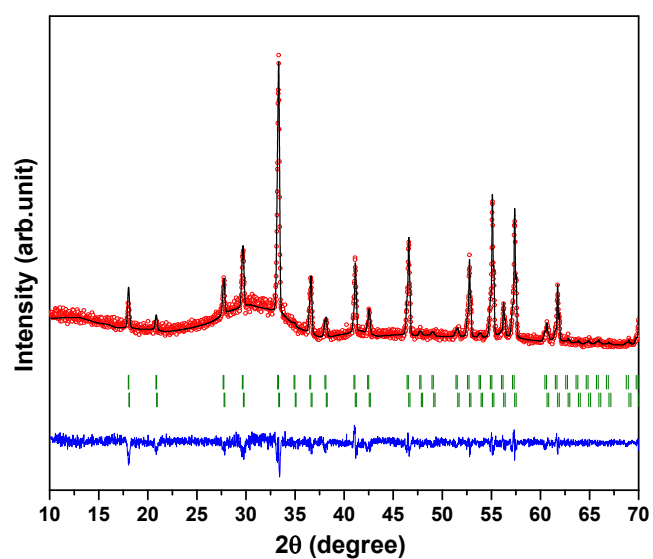


Fig. S3: LeBail refinement plot of $\text{Y}_3\text{Al}_5\text{O}_{12}$ at (a) pristine condition and (b) after irradiated at a fluence of $3 \times 10^{13} \text{ ions/cm}^2$. The vertical lines indicate Bragg positions for cubic garnet.

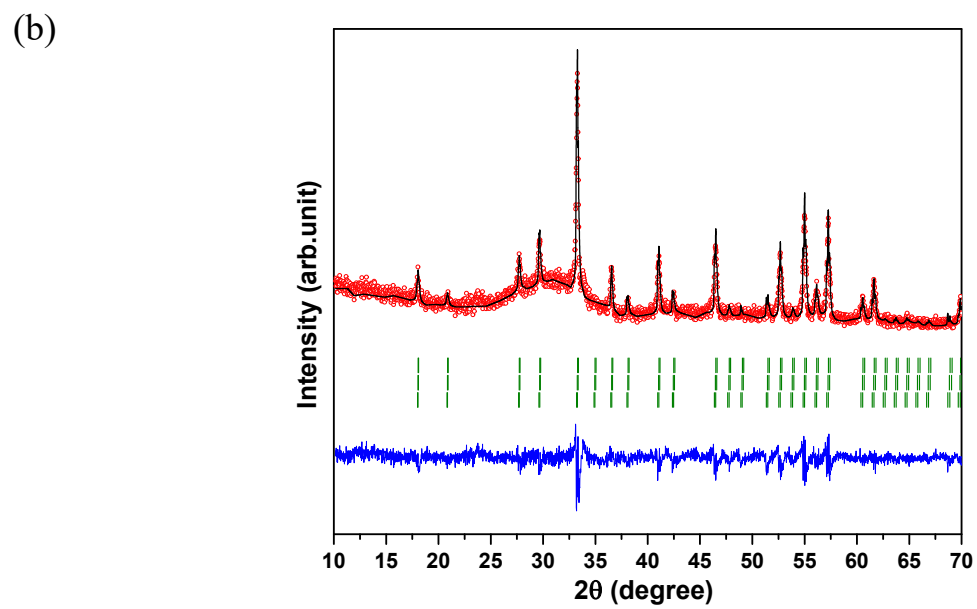
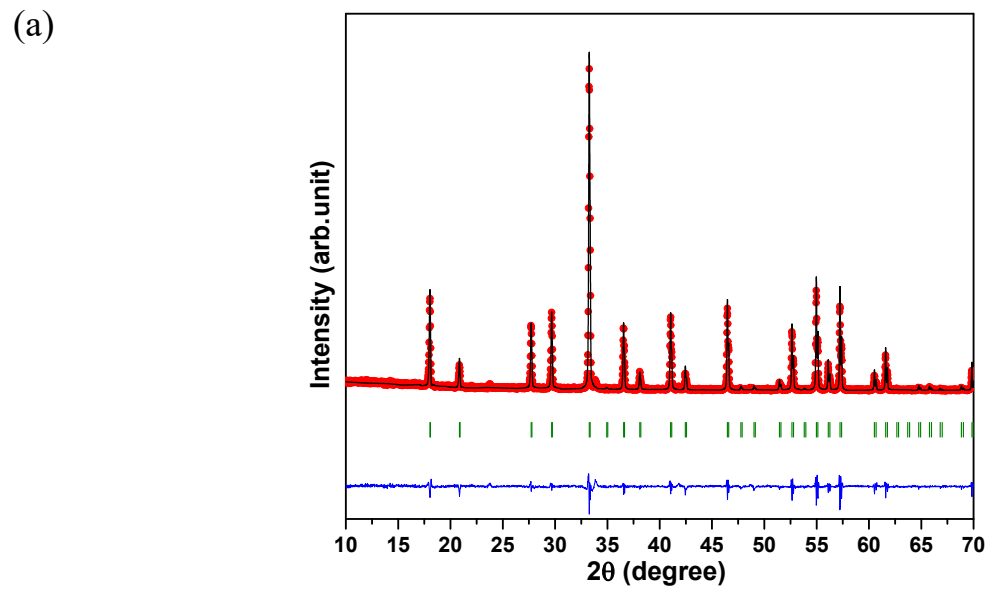


Fig. S4: LeBail refinement plot of $\text{Y}_{2.6}\text{Nd}_{0.4}\text{Al}_5\text{O}_{12}$ at (a) pristine condition and (b) after irradiated at a fluence of 1×10^{13} ions/ cm^2 . The vertical lines indicate Bragg positions for cubic garnet.

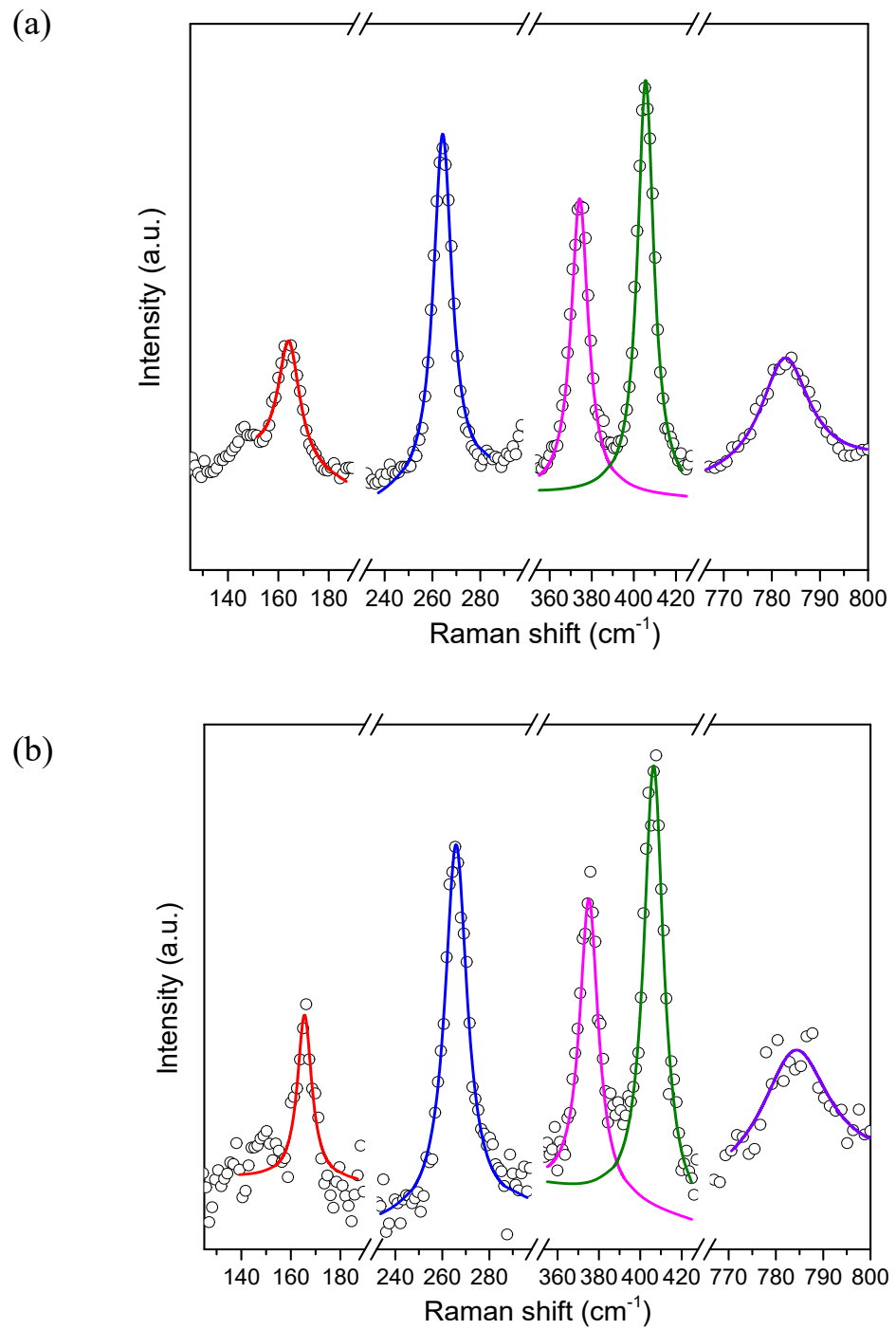


Fig. S5: Representative fitted Raman modes of Nd-YAG at (a) pristine condition and (b) after irradiated at a fluence of 1×10^{13} ions/ cm^2 .

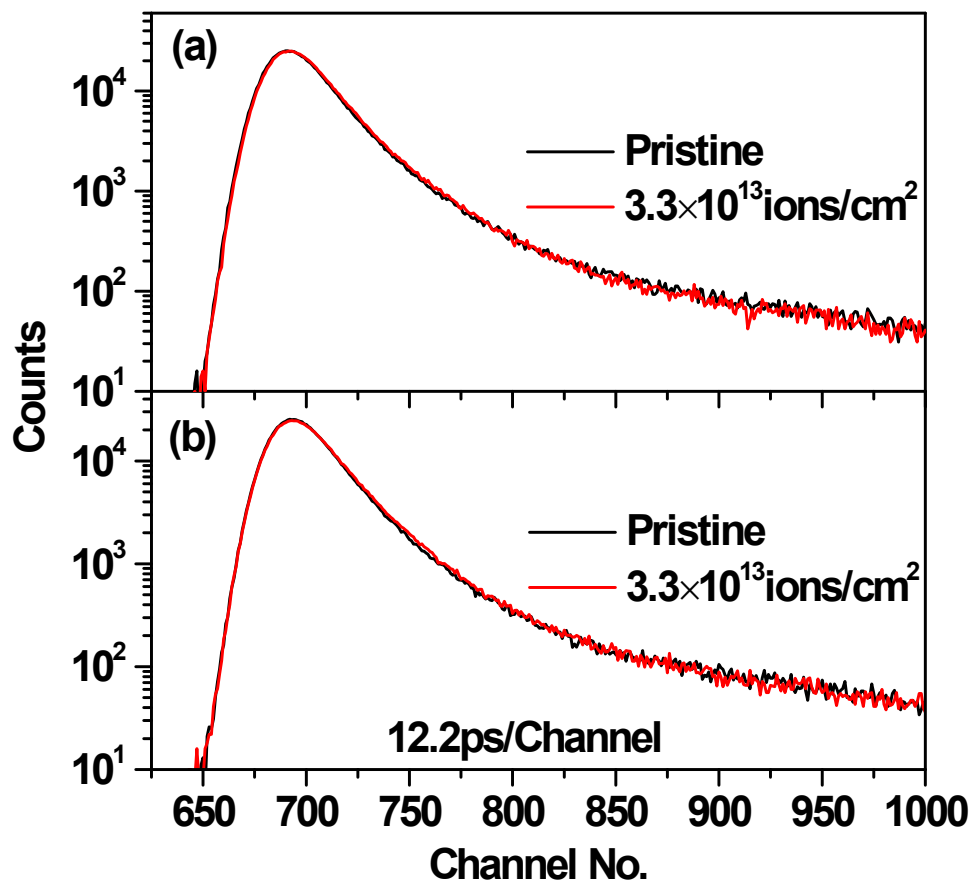


Fig. S6. PALS spectra of (a) YAG and (b) Nd-YAG at pristine and irradiated (at 3.3×10^{13} ions/ cm 2) condition.

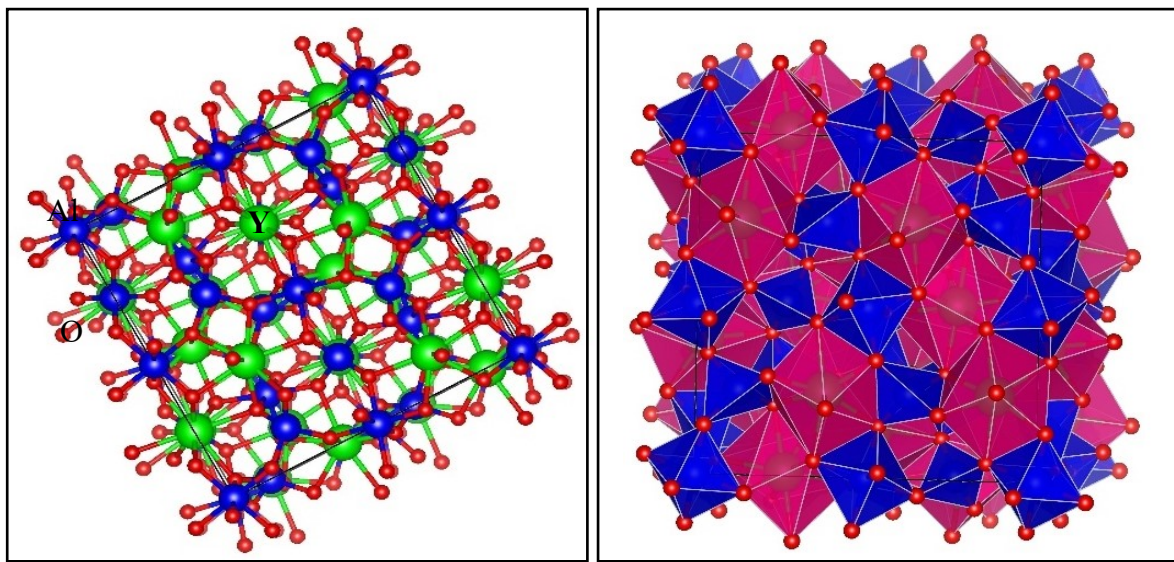


Fig. S7: Crystal structure for $\text{Y}_3\text{Al}_5\text{O}_{12}$. Blue polyhendra indicates AlO_4 and AlO_6 units, while pink polyhendra indicates YO_8 unit.

Table S1: Elemental analysis results of $\text{Y}_3\text{Al}_5\text{O}_{12}$ and $\text{Y}_{2.6}\text{Nd}_{0.4}\text{Al}_5\text{O}_{12}$.

Nominal Composition	Y (atom%)	Nd (atom%)	Al (atom%)
	Determined	Determined	Determined
	(Expected)	(Expected)	(Expected)
$\text{Y}_3\text{Al}_5\text{O}_{12}$	38 (37.5)	-	62 (62.5)
$\text{Y}_{2.6}\text{Nd}_{0.4}\text{Al}_5\text{O}_{12}$	35 (32.5)	5 (5)	60 (62.5)

Table S2: Comparison of Raman frequencies of select modes in unirradiated sample and sample irradiated at 1×10^{13} ions/cm²

Raman Mode for unirradiated sample			Raman Mode for irradiated sample at a fluence of 1×10^{13} ions/cm ²		
Wavenumber (cm ⁻¹)	FWHM (cm ⁻¹)	2σ	Wavenumber (cm ⁻¹)	FWHM (cm ⁻¹)	2σ
164.1	10.6	0.3	165.5	7.1	0.6
264.3	9.4	0.2	265.8	11.5	0.3
374.2	9.9	0.2	375.2	11.0	0.4
405.6	9.4	0.2	406.5	11.6	0.2
782.7	12.3	0.4	784.2	17.3	1.2

σ: standard deviation

Table S3: Measured values of thermal conductivity for YAG and Nd-YAG.

Temperature (K)	Thermal Conductivity (Wm ⁻¹ K ⁻¹)	
	YAG	Nd-YAG
300	7.377	5.081
373	6.054	4.174
473	5.406	3.796
573	4.95	3.432
673	4.602	3.23
773	4.296	3.131
873	4.109	3.086
973	3.845	3.005
1073	3.683	2.865